doi:10.1016/j.jmb.2010.07.006 J. Mol. Biol. (2010) 401, 831–842

JMB

Available online at www.sciencedirect.com

ScienceDirect

ELSEVIER

Ion Selectivity of the KcsA Channel: A Perspective from Multi-Ion Free Energy Landscapes

Bernhard Egwolf and Benoît Roux*

Department of Biochemistry and Molecular Biology, The University of Chicago, Gordon Center for Integrative Science, 929 East 57th Street, Chicago, IL 60637, USA

Received 8 April 2010; received in revised form 2 July 2010; accepted 2 July 2010
Available online 17 July 2010

Potassium (K^+) channels are specialized membrane proteins that are able to facilitate and regulate the conduction of K^+ through cell membranes. Comprising five specific cation binding sites (S_0–S_4) formed by the backbone carbonyl groups of conserved residues common to all K^+ channels, the narrow selectivity filter allows fast conduction of K^+ while being highly selective for K^+ over Na^+. To extend our knowledge of the microscopic mechanism underlying selectivity in K^+ channels, we characterize the free energy landscapes governing the entry and translocation of a Na^+ or a K^+ from the extracellular side into the selectivity filter of KcsA. The entry process of an extracellular ion is examined in the presence of two additional K^+ in the pore, and the three-ion potential of mean force is computed using extensive all-atom umbrella sampling molecular dynamics simulations. A comparison of the potentials of mean force yields a number of important results. First, the free energy minima corresponding to configurations with extracellular K^+ or Na^+ in binding site S_0 or S_1 are similar in depth, suggesting that the thermodynamic selectivity governed by the free energy minima for those two binding sites is insignificant. Second, the free energy barriers between stable multi-ion configurations are generally higher for Na^+ than for K^+, implying that the kinetics of ion conduction is slower when a Na^+ enters the pore. Third, the region corresponding to binding site S_2 near the center of the narrow pore emerges as the most selective for K^+ over Na^+. In particular, while there is a stable minimum for K^+ in site S_2, Na^+ faces a steep free energy increase with no local free energy well in this region. Lastly, analysis shows that selectivity is not correlated with the overall coordination number of the ion entering the pore, but is predominantly affected by changes in the type of coordinating ligands (carbonyls *versus* water molecules). These results further highlight the importance of the central region near binding site S_2 in the selectivity filter of K^+ channels.

Keywords: membrane channel; selectivity; umbrella sampling; molecular dynamics simulation

Edited by D. Case

Introduction

Potassium (K^+) channels belong to a large and diverse group of membrane proteins that are of vital importance to living organisms. The physiological function of these specialized ion channels is to facilitate and regulate the conduction of K^+ through the cell membrane.[1] A most remarkable feature of K^+ channels is their ability to discriminate K^+ over Na^+ by more than a thousandfold while maintaining a fast throughput rate near the diffusion limit.

A first view of the overall molecular architecture of K^+ channels was provided by X-ray structures of the bacterial KcsA channel from *Streptomyces*

*Corresponding author. E-mail address: roux@uchicago.edu.

Present address: B. Egwolf, Department of Theoretical and Computational Biophysics, Max Planck Institute for Biophysical Chemistry, Am Faßberg 11, 37077 Göttingen, Germany.

Abbreviations used: FEP/MD, free energy perturbation/molecular dynamics; PMF, potential of mean force; MD, molecular dynamics; PDB, Protein Data Bank; 3D, three-dimensional; 2D, two-dimensional.

lividans.[2,3] In particular, the X-ray structures revealed the presence of multiple dehydrated K^+ coordinated by main chain carbonyl groups disposed along the narrowest region of the channel, the "selectivity filter," formed by the highly conserved sequence TTVGYGD common to all K^+ channels.[4,5] On the basis of these structural results, the high selectivity for K^+ over Na^+ was explained by pointing out that the carbonyl ligands along the selectivity filter provide a coordination structure perfectly adapted to K^+, but that Na^+ are too small to fit well into the sites.[2,6] While this explanation is consistent with the results of X-ray crystallography,[2,3] numerous computational studies based on atomic models highlighted the fluctuating and dynamic nature of the pore,[7–15] suggesting that the origin of ion selectivity could be more complex (for reviews, see Sansom *et al.*,[16] Roux,[17] and Noskov *et al.*[18]).

In simple terms, the concept of a selective K^+ channel means that the "correct" ion K^+ is able to permeate through the pore more easily than an "incorrect" ion such as Na^+. At the physical level, energetics and solvation are anticipated to play a key role in making the conduction process more unfavorable for Na^+ than for K^+, although different aspects of energetics may be highlighted by various experimental methods used to probe the system. Some experimental measurements are more sensitive to the relative depth of free energy wells, while others are more sensitive to the relative height of free energy barriers.[1] Bi-ionic reversal potential experiments provide information about ion selectivity by considering a nonequilibrium situation with K^+ and Na^+ fluxes running in opposite directions through the channel. However, characterizing the selectivity of a very selective channel quantitatively using this method can be difficult. In the case of the KcsA K^+ channel, measurements indicate that the K^+/Na^+ permeability ratio is greater than 150.[19,20] This can be translated into free energy for Na^+ in the pore that is unfavorable, relative to K^+, by at least 3 kcal/mol (minimum), but it could be more. Ba^{2+} blockade experiments make it possible to assess selectivity more quantitatively.[21,22] Monitoring the K^+ and Na^+ concentration dependence of Ba^{2+} blockades, it is possible to accurately measure the relative binding free energy of those two ions in specific sites under near-equilibrium conditions. Using this strategy, Neyton and Miller discovered a K^+ binding site in the selectivity filter, which they called the "external lock-in site," and estimated the binding free energy of Na^+ in this site to be about +5.5 kcal/mol relative to K^+. Comparison with X-ray crystallographic results suggests that the external lock-in site is probably some amalgam of the S_2 and S_1 sites.[23,24] Consistent with these experimental observations, thermodynamic free energy perturbation/molecular dynamics (FEP/MD) simulations have shown that sites S_1 and S_2 are the most selective.[11,12,15] Nonequilibrium punch-through experiments, carried out in the presence of intracellular Na^+, can also provide quantitative information about the magnitude of the free energy barriers encountered by Na^+ or Li^+ for crossing the selectivity filter.[25,26] The measurements yield S-shaped current–voltage curves with a local minimum, which reflect a voltage-dependent block that is relieved at high positive voltage as the forward escape of the blocker through the selectivity filter is accelerated. Brownian dynamics trajectories using the multi-ion potential(s) of mean force (PMF) calculated from all-atom molecular dynamics (MD) simulations[11,27] suggested that the Na^+ punch-through measurements are consistent with the passage of one Na^+ being opposed by a free energy barrier of about 5–6 kcal/mol centered on binding site S_2.[18]

Selectivity can also be examined under strict conditions of thermodynamic equilibrium using differential microcalorimetry, whereby ion binding is detected as the channel is exposed to a solution containing K^+ or Na^+ at various concentrations.[24] Those experiments can be interpreted in the light of X-ray crystallography results showing that the selectivity filter adopts a different conformation in the presence or in the absence of K^+.[3,24] At high K^+ concentration [Protein Data Bank (PDB) ID 1K4C], the filter simultaneously binds at least two K^+ in four discrete sites (S_1–S_4) and adopts what is thought to be a conductive state. At a high concentration of Na^+ and a very low concentration of K^+ (PDB ID 1K4D), the filter is narrowed at the level of Val76-Gly77 and binds a single K^+ in either site S_1 or site S_4. This so-called low-K^+ conformation (also referred to as "pinched" or "collapsed") is believed to be nonconductive. This is confirmed by MD simulations indicating that the low-K^+ conformation is not permeable by K^+.[28] Consistent with this, PMF calculations indicate that even a partly collapsed filter with only a single flipped Val76-Gly77 carbonyl group would be sufficient to undermine the conduction of K^+.[29] The transition from a conductive conformation to a collapsed conformation of the KcsA, which is possibly related to the process called C-type inactivation,[28,30–32] reveals one important aspect of ion selectivity in the KcsA channel. A tantalizing interpretation from those observations could be that the conductive–nonconductive conformation change in the filter is the actual phenomenon that underlies the selectivity of K^+ channels: the filter adopts a conductive conformation when occupied by K^+, and collapses and stops conducting as it becomes occupied by Na^+. However, it is important to realize that the mechanism of selective ion transport through the open conductive channel and the conformational change in the filter driven by K^+ binding may be two different, albeit related, phenomena. For instance, in X-ray studies, the collapsed state is observed at a very low concentration or in the complete absence of K^+. Furthermore, the conductive-to-collapsed conformation change takes place on a relatively slow timescale,[24] and one would expect that, when the filter conducts ions at a high rate in bi-ionic flux

experiments, it will remain in its conductive conformation as K^+ (and a few Na^+) flow through. This view is further supported by the observation that a synthetic KcsA channel with a D-alanine substituted at the position of Gly77 does not collapse at low K^+ concentration and remains nonetheless selective for K^+ over Na^+ in functional measurements.[33] Those results show that the KcsA channel is selective for K^+ over Na^+, even as the pore remains in the conductive conformation.

In this regard, it is useful to recall the biological context in which the high selectivity of K^+ channels is called into play. Voltage-gated K^+ channels in nerve cells are activated to allow the passive outward current of K^+ from the intracellular side, where their concentration is around 160 mM, to the extracellular side, where their concentration is about 2–4 mM. An important purpose of the highly selective permeability to K^+ is to restore the resting membrane potential of the cell after the nerve impulse. During this activity, it is critical that the open K^+ channels be able to oppose the inward passage of Na^+, which are very abundant on the extracellular side, down their electrochemical potential. Under physiological conditions, the selectivity filter is primarily occupied by K^+ and is probably in its conductive conformation. To permeate, an undesired Na^+ must enter the conductive selectivity filter from the extracellular side and continue to transit into the pore toward the intracellular side in the presence of K^+. The primary event for this process must be the translocation of a Na^+ from site S_0 to site S_1, then to site S_2, and so on and so forth. The sequence of multi-ion configurations that must be visited is illustrated schematically in Fig. 1.

Ion movements during the inward conduction process are expected to take place in a highly concerted fashion, as the ions in the pore undergo transitions between different multi-ion configurations of the five cation binding sites S_0–S_4. While FEP/MD simulations have shown that the selectivity for K^+ over Na^+ varies along the selectivity filter, reaching a maximum (5–6 kcal/mol) near the central site S_2,[11,15] such calculations reflect the relative free energies of Na^+ and K^+ within the wells. Furthermore, FEP/MD calculations probe ion selectivity "punctually" for specific ion configurations in the binding sites. They do not address the height of free energy barriers, as well as the kinetic and dynamic aspects of selectivity. Key issues are, for example, how far an undesired Na^+ is able to wander into the pore before it is repelled, and which specific parts of the selectivity filter play a crucial role during those events. For this reason, it is important to determine not only the relative stability of binding sites but also the free energy barriers between them.

The goal of this study is to extend our understanding of ion selectivity by characterizing the free energy landscapes governing the entry and translocation of a Na^+ or a K^+ into the filter from the extracellular side. The best strategy to address such issues is to compute the multi-ion PMF corresponding to the microscopic process in question.[11] In particular, the calculation of the PMF enables us to pinpoint the location of the largest barrier opposing the passage of a single Na^+ while there are two K^+ elsewhere in the pore. The PMF for this 3-ion process was computed using three-dimensional (3D) umbrella sampling MD simulations and compared with the corresponding PMF for three K^+. In the next section, the results of the computations are discussed. A brief conclusion highlighting the main points follows. Afterwards, the atomic simulation system and the computational methodology are described.

Results and Discussion

A powerful computational strategy to understand the long-time dynamics governing ion conduction through K^+ channels consists of representing the evolution of permeating ions in terms of a random stochastic Brownian motion taking place on an effective free energy surface given by the multi-ion PMF.[34] Such a PMF-based framework finds its roots in statistical mechanical theories of nonequilibrium transport phenomena in which dissipative equations of motion are derived for a reduced set of degrees of freedom while projecting out the dynamics of the rest of the system (see Zwanzig[35] and references therein). The most crucial ingredient entering the construction of such a reduced stochastic model is the multi-ion PMF. The latter is an effective configuration-dependent free energy surface,[36] which directly controls all the underlying equilibrium structural properties arising from the effective stochastic dynamics. Furthermore, the gradient of the PMF is related to the average (mean) force acting on the ions,[34] and the lowest energy pathway dictates the long-time dynamics.[27]

The PMF-based strategy was used previously to characterize the conduction of K^+ through the KcsA channel.[11,27] The calculations showed that K^+ could be located in five energetically favorable binding sites along the selectivity filter (S_0–S_4),[11] in accord with the results from high-resolution X-ray crystallography.[3,37] Furthermore, the calculated

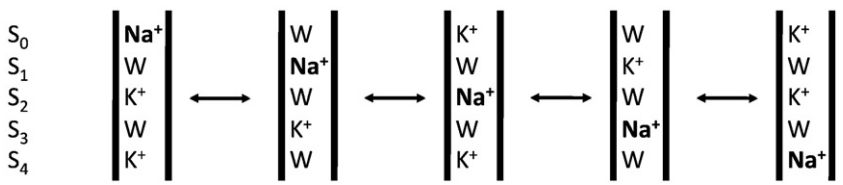

Fig. 1. Schematic illustration of the sequence of events needed for the entry of one Na^+ from the extracellular side into the selectivity filter of the channel filled with K^+ and water molecules (W).

PMF revealed that the lowest energy pathway for the multi-ion conduction process was similar to the "knock-on" mechanism originally proposed by Hodgkin and Keynes, in which an incoming K^+ collides and pushes the single file of ions through the narrow pore $K^+\cdots[K^+, K^+]\rightarrow[K^+, K^+]\cdots K^+$.[38] Specifically, the concerted transition $[S_4, S_3, S_1]\leftrightarrow[S_4, S_2, S_0]$ was seen to play a critical role for both outward conduction and inward conduction of K^+. Recent results extracted from long unbiased microsecond MD trajectories of an atomic model of the Kv1.2 channel embedded in a solvated membrane confirmed the mechanistic conclusions about ion conduction drawn from the PMF-based strategy.[39]

Here, the PMF-based strategy is extended to compare the entry of a Na^+ ($Na^+/K^+/K^+$ system) and the entry of a K^+ ($K^+/K^+/K^+$ system) into the filter from the extracellular side of the channel. It is emphasized that the multi-ion PMF-based strategy does not impose any specific steps during the translocation process considered here. The configuration of the single file of ions is properly sampled, and the most probable sequence of microscopic events during the translocation process is an outcome of the free energy surface. The outermost ion (K^+ or Na^+) is called ion I_1 throughout the text. A special configuration of the ions in the $Na^+/K^+/K^+$ system is shown in Fig. 2. Ion I_1 is the ion closest to the extracellular side of the selectivity filter. Ions I_2 and I_3 (K^+ in both systems) are located farther inside the channel pore than ion I_1 (Fig. 2, middle and lower ions). In the selectivity filter, two neighboring ions are separated by a water molecule.[9,11] The umbrella sampling calculations follow the multi-ion inward conduction process, tracking the entry of the outermost ion I_1 from the extracellular side all the way to the region of the central binding site S_2 in the selectivity filter. It is not possible to draw conclusions about the permeation process beyond this configuration because the intracellular gate of the KcsA channel is closed (the ion in the cavity cannot leave to the intracellular side). For this reason, ion I_3 cannot leave the cavity, and site S_2 is the most inward location that can be reached by ion I_1. In spite of this limitation, the computed 3D PMF of the $K^+/K^+/K^+$ and $Na^+/K^+/K^+$ systems provide new quantitative information about the complex free energy landscape governing ion selectivity and permeation in KcsA K^+ channels.

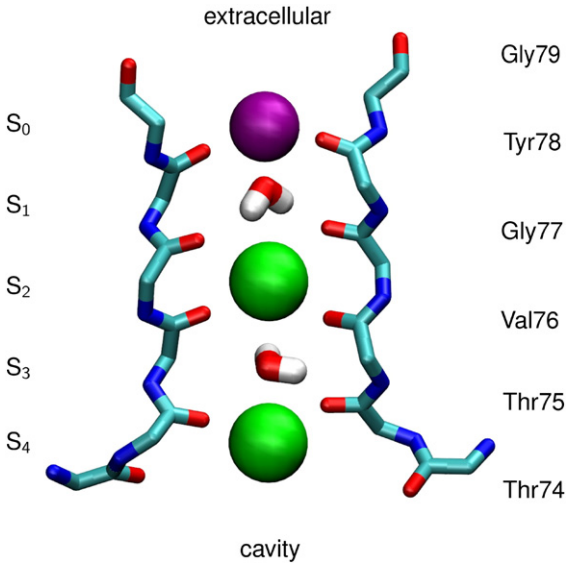

Fig. 2. Instantaneous MD simulation structure of the selectivity filter of KcsA occupied by one Na^+ and two K^+ in the configuration $[S_0, S_2, S_4]$. This structure belongs to the $Na^+/K^+/K^+$ system, whereas the $K^+/K^+/K^+$ system has three K^+ in the selectivity filter region (structure not shown). For clarity, only backbone atoms of the residues forming the selectivity filter are displayed, and two of four monomers are omitted. The corresponding residue names are listed on the right. Above the selectivity filter is the extracellular side of the channel, and below the selectivity filter is a cavity filled with water molecules. Na^+ (ion I_1; purple sphere) occupies binding site S_0 at the extracellular entrance. The two K^+ (I_2 and I_3; green spheres) are located in binding sites S_2 and S_4. Each of the binding sites S_1 and S_3 is occupied by a single water molecule separating the ions in the selectivity filter. The image was produced using the program VMD.[40]

The 3D PMFs are projected on coordinates Z_1 (location of K^+ or Na^+) and Z_{23}, which is the mean of positions Z_2 and Z_3 of the two lower K^+ according to Eq. (1), to facilitate visualization and analysis. The resulting two-dimensional (2D) PMF are shown in Fig. 3 as contour plots. Neighboring contour levels differ by 1 kcal/mol; the energy scale goes from black (low energy) to red (high energy). The blank areas in the various maps correspond to high energy multi-ion configurations that were not explored by umbrella sampling window simulations to reduce the computational cost of the calculations. Three instantaneous configurations—(a), (b), and (c)—taken from the MD simulations and pointing to different areas in the maps are used to illustrate the progress of the multi-ion transition process in the selectivity filter of the $K^+/K^+/K^+$ and $Na^+/K^+/K^+$ systems.

We first discuss the results for the $K^+/K^+/K^+$ system. In configuration (a), the three K^+ initially occupy sites S_0, S_2, and S_4. In configuration (b), the two outermost K^+ move toward sites S_1 and S_3, while the innermost K^+ leaves site S_4 to enter the cavity region. Finally, in configuration (c), the two outermost K^+ occupy sites S_2 and S_4, and the innermost K^+ is in the cavity. For the $Na^+/K^+/K^+$ system, the configurations are similar, although there are some slight differences, because Na^+ does not rest at the center of the binding sites, like K^+, due to its smaller size. In configuration (a), the two inner K^+ are in sites S_2 and S_4, while the outer Na^+ is in site S_0. The position of Na^+ is slightly more inward than when a K^+ occupies site S_0, to be more precise. In configuration (b), the outer Na^+ is also in an inwardly displaced site S_1, while the central K^+ is in site S_3 and the innermost K^+ leaves site S_4 to enter the cavity region. Finally, in configuration (c), the outer Na^+ is in site S_2, while the two innermost K^+ are in site S_4 and in the cavity.

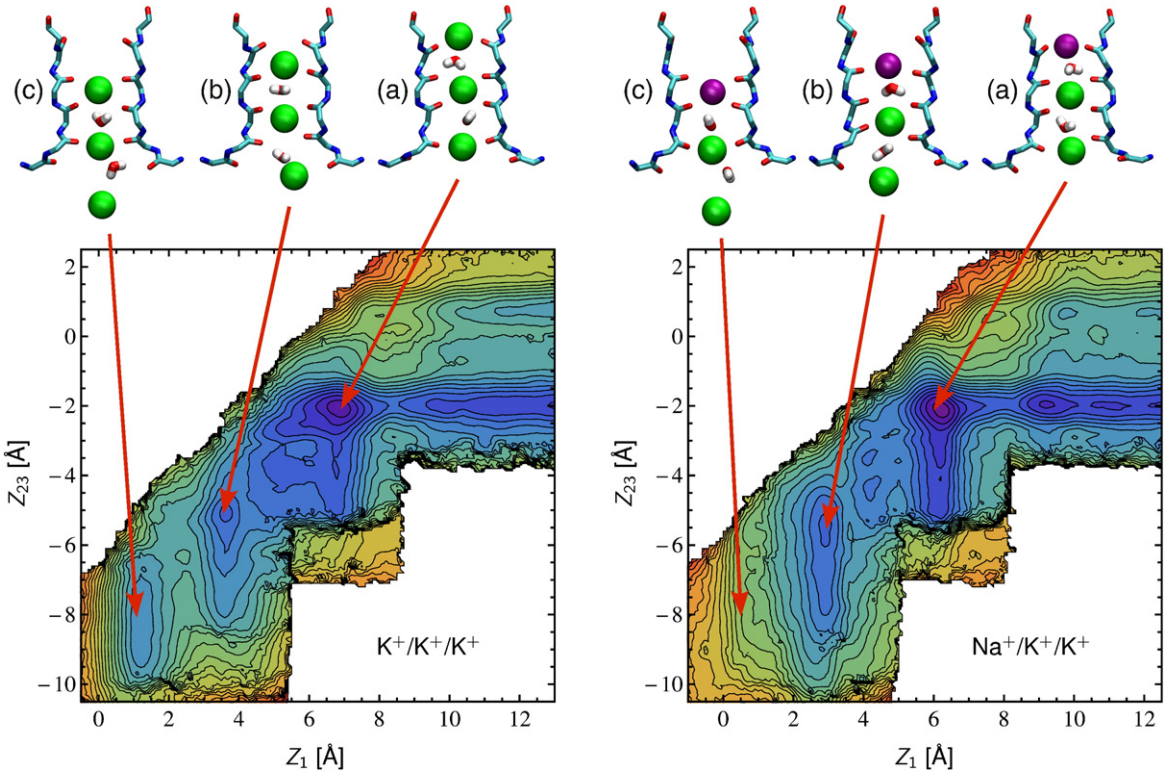

Fig. 3. Contour plots of 2D PMF calculated from the 3D PMF of the $K^+/K^+/K^+$ system (left PMF), with solely K^+ in the selectivity filter, and of the $Na^+/K^+/K^+$ system (right PMF), where one K^+ is replaced by a Na^+. Two neighboring contour levels differ by 1 kcal/mol. Low energy regions are depicted in blue, and high energy regions are depicted in red. Coordinate Z_1 is the position of ion I_1 (K^+ or Na^+) along the Z-axis of the system, which is parallel with the pore formed by the selectivity filter. The 3D PMF are projected on 2D PMF with coordinates Z_1 and Z_{23}, according to Eq. (1). Coordinate Z_{23} is the mean of the respective positions Z_2 and Z_3 of the two lower K^+. The zero position along the Z-axis of the system is defined by the center-of-mass of the backbone atoms of residues Thr75, Val76, Gly77, and Tyr78 (see Fig. 2). A comparison of both PMF shows that the energy well at the lower left corner of the $K^+/K^+/K^+$ system PMF has no counterpart in the $Na^+/K^+/K^+$ system PMF. Instantaneous snapshots taken from the MD simulations are used to illustrate the configuration of the ions in the selectivity filter for selected areas in the contour plots: (a) [S_0, S_2, S_4], (b) [S_1, S_3, cavity], and (c) [S_2, S_4, cavity]. The selectivity filter images were produced using the program VMD.[40]

The upper right area of the two PMF shown in Fig. 3 corresponds to the process of the outer ion I_1 (K^+ or Na^+) entering binding site S_0 from the extracellular side of the channel. The process takes place in the presence of two K^+ in the selectivity filter. The configuration [S_0, S_2, S_4] (with ion I_1 in binding site S_0, ion I_2 in binding site S_2, and ion I_3 in binding site S_4) depicted in (a) corresponds to the deep free energy well. In the $K^+/K^+/K^+$ system, this free energy well is located roughly at $Z_1 = 7$ Å, whereas the corresponding minimum in the $Na^+/K^+/K^+$ system is at $Z_1 = 6$ Å. In the Z_{23} direction, the energy well is at -2 Å in both systems. That is, the distance of ion I_1 (K^+ or Na^+) to the other two ions is larger in the $K^+/K^+/K^+$ system than in the $Na^+/K^+/K^+$ system. This reflects the fact that Na^+ is smaller in size than K^+, and that it binds closer to the carbonyl oxygens of the selectivity filter. In the $Na^+/K^+/K^+$ system, the free energy well extends more downwards, parallel with the Z_{23} axis, than the corresponding free energy well in the $K^+/K^+/K^+$ system. This means that Na^+ tends to remain "locked" in binding site S^0, while the system allows the inner K^+ I_2 and I_3 to move deeper into the channel. In contrast, the free energy landscape in the $K^+/K^+/K^+$ system seems to favor the concerted multi-ion translocation of all three K^+ in the filter.

The next step is the transition of ion I_1 to S_1, ion I_2 to S_3, and ion I_3 to the central cavity. The latter situation [S_1, S_3, cavity] is illustrated by configuration (b) of Fig. 3. Associated with this configuration is a free energy well in the PMF of the $K^+/K^+/K^+$ and $Na^+/K^+/K^+$ systems. It is particularly noteworthy that the free energy difference between configurations (a) and (b) for the $K^+/K^+/K^+$ system and the free energy difference between configurations (a) and (b) for the $Na^+/K^+/K^+$ system are very similar. The implication from Fig. 3 is that there is no significant extra free energy cost for moving a Na^+ from site S_0 to site S_1, compared to moving a K^+ over the same sites. While this observation may appear surprising, it is consistent with the results of FEP/MD simulations indicating that the outermost binding sites are not very selective for K^+ over Na^+.[11,15] Also consistent with this conclusion, spontaneous entry into the pore of a Na^+ placed near the extracellular entrance was observed by unbiased MD trajectories.[7]

When the ions move further inward into the selectivity filter, they reach the lower left area of the PMF in Fig. 3. In this configuration, there is an extended free energy well in the PMF of the $K^+/K^+/K^+$ system, corresponding to a situation depicted in (c), with ion I_1 in S_2, ion I_2 in S_4, and ion I_3 in the cavity. There is no such free energy well in the corresponding area of the PMF calculated for the $Na^+/K^+/K^+$ system. Instead, a steep increase in free energy, which prevents Na^+ from moving deeper into the pore, is observed. Figure 4 shows the free energy landscape corresponding to a transition from (b) to (c) in sharper detail, as ion I_1 goes from S_1 to S_2 and as ion I_2 goes from S_3 to S_4. Here, the multi-ion translocation is followed on PMF free energy maps calculated as projections of the 3D PMF on coordinates Z_1 and Z_2 according to Eq. (2). Those are the most relevant coordinates because ion I_3 is not in the selectivity filter anymore, but in the central cavity of the channel. Therefore, coordinate Z_3 could be integrated out without losing much information. A comparison of the two PMF in Fig. 4 shows again that the energy well at the lower left corner of the $K^+/K^+/K^+$ system PMF has no counterpart in the $Na^+/K^+/K^+$ system. Instead, the inward movement of Na^+ is opposed by a steep increase in free energy, near the region corresponding to binding site S_2. The map shows that, in this situation, S_2 is not a binding site for Na^+. The free energy well in the PMF of the $Na^+/K^+/K^+$ system again displays some downwards extension, parallel with the Z_2 axis. This means that the Na^+ I_1 is blocked at the level of S_1 and is unable to move to S_2, while the K^+ I_2 is able to translocate to binding site S_4. This is in stark contrast with the $K^+/K^+/K^+$ system, where K^+ I_1 and I_2 are able to make a concerted transition toward sites S_2 and S_4, respectively.

Because of the relatively high complexity of the PMF governing the multi-ion transitions in terms of the Z-position of the three ions in the selectivity filter, it is helpful to consider various projections onto smaller subsets of degrees of freedom. At the simplest level, Fig. 5 displays one-dimensional projections of the 3D PMF on the Z_1 axis for the $K^+/K^+/K^+$ and $Na^+/K^+/K^+$ systems. Here, coordinates Z_2 and Z_3 were integrated out according to Eq. (3). While such an effective one-ion "free energy

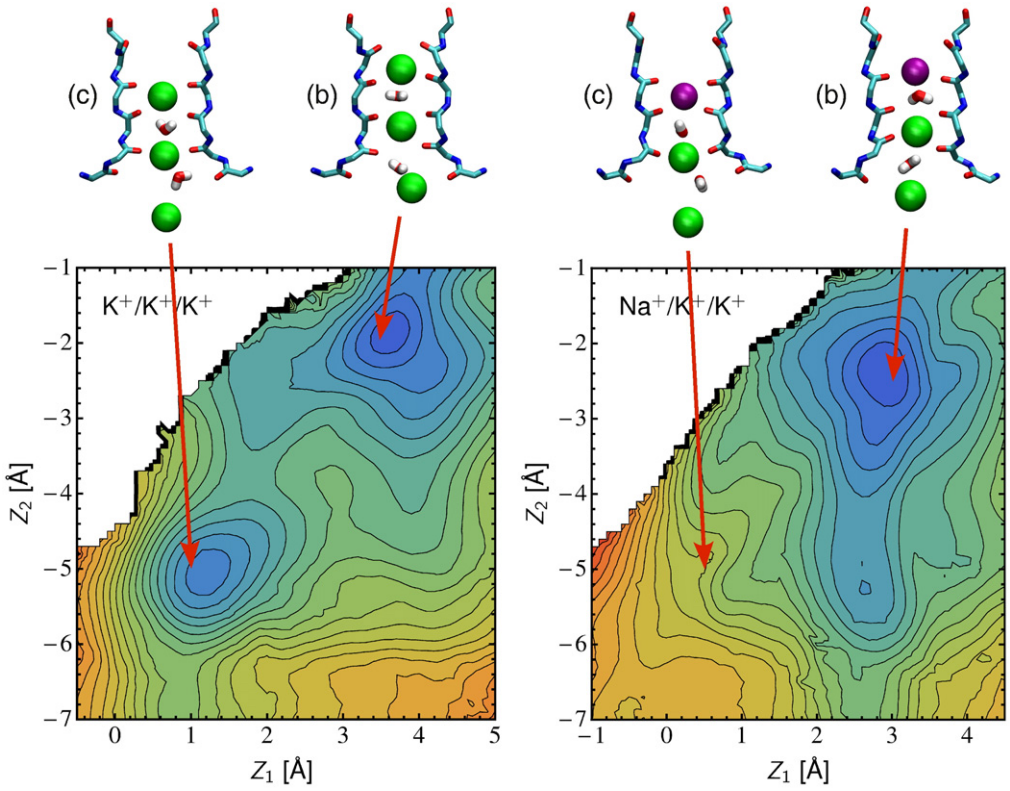

Fig. 4. Contour plots of 2D PMF calculated from those regions of the 3D PMF that belong to the lower left areas in the contour plots of Fig. 3. Two neighboring contour levels differ by 1 kcal/mol. Low energy regions are depicted in blue, and high energy regions are depicted in red. The 3D PMF are projected on 2D PMF with coordinates Z_1 and Z_2, according to Eq. (2). These are the most relevant coordinates in this region because only ion I_1 [i.e., K^+ (left PMF) or Na^+ (right PMF)] and ion I_2 are in the selectivity filter, whereas ion I_3 is already in the cavity. Images of instantaneous MD simulation snapshots show the location of the ions relative to the selectivity filter for selected areas of the contour plots: (b) [S_1, S_3, cavity] and (c) [S_2, S_4, cavity]. There are two energy wells in the $K^+/K^+/K^+$ system PMF, but only one in the $Na^+/K^+/K^+$ system PMF. The lower left energy well in the $K^+/K^+/K^+$ system PMF belongs to a situation where ion I_1 is located at binding site S_2 (see snapshot (c)). The corresponding area of the $Na^+/K^+/K^+$ system PMF shows a steep energy increase instead. The selectivity filter images were produced using the program VMD.[40]

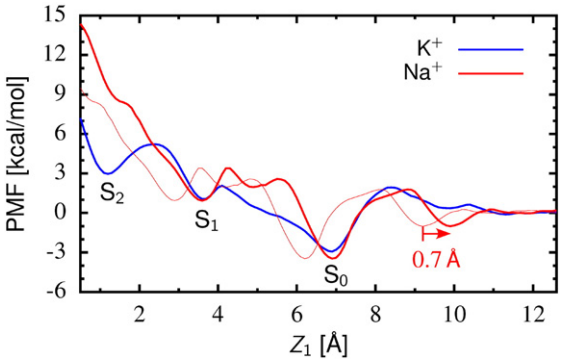

Fig. 5. One-dimensional PMF for coordinate Z_1 (K^+ or Na^+) calculated from the 3D PMF according to Eq. (3). The Na^+ Z_1 coordinate is shifted by 0.7 Å relative to the K^+ Z_1 coordinate. This overlays the main minima of the PMF and makes it easier to compare them. The $K^+/K^+/K^+$ system PMF has energy minima at the positions of binding sites S_0, S_1, and S_2. The $Na^+/K^+/K^+$ system PMF has energy minima at the positions of binding sites S_0 and S_1, whereas no comparable minima can be found where binding site S_2 would be expected.

profile" (in terms of the Z position of the outermost ion) is the most reductive projection of the complex 3D PMF, it provides the most direct view of the free energy landscape governing the entry of a K^+ or a Na^+ into the selectivity filter of the KcsA channel from the extracellular side. The features of the one-ion PMF summarize the critical steps for the permeation of K^+ and Na^+ from the extracellular side. Interestingly, the wells for and barriers to K^+ and Na^+ are not quite located at matching positions. Bindings sites S_0 and S_1 for the smaller Na^+ are shifted by about 0.7 Å with respect to those for K^+. It is possible to provide a simple geometrical explanation of the relative shift between Na^+ and K^+, consistent with the observation that the selectivity filter is not distorted significantly regardless of the permeating cation. The contact distance between K^+ and the backbone carbonyl oxygens is about 2.8 Å, while the corresponding contact distance with Na^+ is about 2.4 Å. As an ion rests in contact with the carbonyl oxygen along the pore axis, it is located at the position $Z_i = \sqrt{R_{io}^2 - (R_{oo}/2)^2}$, where R_{io} is the ion–carbonyl contact distance, and R_{oo} is the carbonyl–carbonyl distance. The latter is about 4.2 Å for opposite subunits across the selectivity filter, yielding a shift $Z_K - Z_{Na}$ of about 0.7 Å along the Z-axis between Na^+ and K^+. To make the comparison of the two systems easier, the PMF of Na^+ was shifted by 0.7 Å along the Z-axis, resulting in an overlay of the free energy minima of the PMF. At the outer end of the PMF, where ion I_1 enters the selectivity filter, there is a clear free energy minimum for Na^+, but only a very shallow one for K^+. This is due to the interactions of the ions with the extracellular entrance of the selectivity filter. The relative free energy difference of the minima at S_0 and S_1 is only slightly larger for Na^+ than for K^+. However, Na^+ has to overcome a higher barrier with a shallow intermediate free energy minimum in order to transit from S_0 and S_1. The same transition appears much smoother for K^+. Importantly, the effective free energy profile for K^+ has a local minimum at binding site S_2, which is not present in the case of Na^+. That is, Na^+ encounters the highest repulsive barrier as it attempts to make the inward transition from S_1 to S_2.

The absence of a stable location for Na^+ in binding site S_2 has important implications for alchemical FEP/MD studies of ion selectivity in the KcsA channel. Long unrestricted FEP/MD simulations during which a K^+ is transformed into a Na^+ should, in principle, allow the entire system to sample all possible configurations. However, unrestricted FEP/MD simulations attempting to transform a K^+ located in site S_2 into a Na^+ may run into problems, as the system will try to evolve toward a different favorable state at the end point of the alchemical transformation. The free energy difference $\Delta G_{Na,K}$ obtained from such unrestricted FEP/MD may not necessarily yield useful information about permeation, particularly when K^+ and Na^+ binding sites have different locations, or may not even coexist altogether. In this sense, it is important to recall that the central quantity governing ion conduction and selectivity is the free energy landscape provided by the multi-ion PMF $W(Z_1, Z_2, Z_3)$ for K^+ and Na^+, not the relatively simple $\Delta\Delta G_{Na,K}$. To avoid some of those problems, it is possible to utilize the FEP/MD simulations to make "punctual" measurements of the underlying PMF by ensuring that the Z position of the ions in the selectivity filter is restricted in specific multi-ion configurations[15] (e.g., the transformation of a K^+ into a Na^+ in site S_2 must be evaluated as $\Delta G^{rest}_{Na,K} \equiv [W_{K/Na/K}(Z_1, Z_2, Z_3) - W_{K/K/K}(Z_1, Z_2, Z_3)]$).

It is of interest to see how the features of the one-ion free energy profile shown in Fig. 5 relate to variations in the coordination structure around the ion as it enters into the selectivity filter. The average number of coordinating oxygen from backbone carbonyls or water molecules around the K^+ and Na^+ calculated from additional simulations is shown in Fig. 6. As expected, the number of coordinating water molecules decreases as the ion moves from the bulk phase into the narrow selectivity filter, for $Z_1 < 7$ Å. However, the total coordination number displays only small variations: over the entire entry process, the average coordination number of K^+ increases slightly from 6 to 7, while that of Na^+ remains constant around 5.5. Thus, selectivity in KcsA does not appear to be correlated with the total coordination number of the ion entering the pore. Considering the free energy profile shown in Fig. 5, the increase in selectivity for K^+ over Na^+ that is observed near site S_2 seems to be mostly associated with a decrease in the average number of coordinating water molecules around the ion. For K^+, there is a progressive substitution of water by backbone carbonyl ligands over a distance of almost 6 Å (for 4 Å $< Z_1 <$ 10 Å). Once K^+ is deeper into the filter, the average number of coordinating

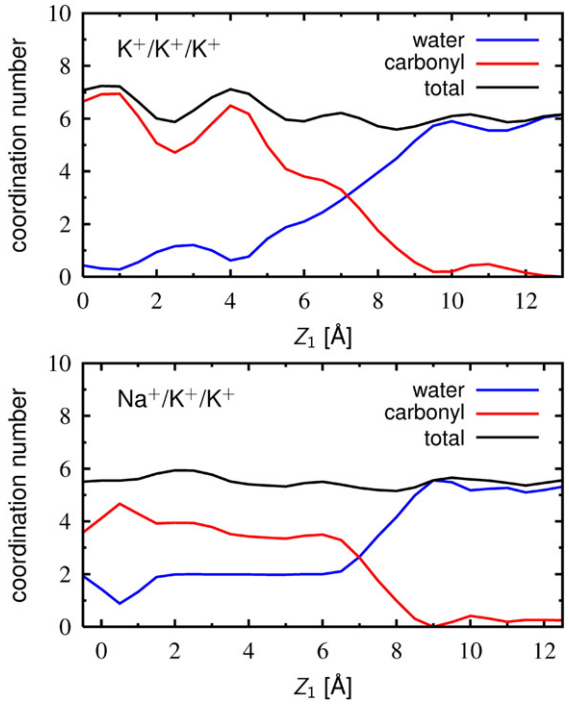

Fig. 6. Average coordination numbers for ion I_1 at different ion positions Z_1 for special paths in the 3D PMF landscapes. The average numbers of water, carbonyl, and total oxygen atoms, which are not farther away than 3.2 Å from ion I_1 in the $K^+/K^+/K^+$ system and not farther away than 2.8 Å in the $Na^+/K^+/K^+$ system, are shown.

water molecules around the ion is smaller than 1. For Na^+, the substitution of coordinating ligands takes place over a shorter distance, about 4 Å (for 6 Å$<Z_1<$10 Å). Interestingly, the average number of water molecules around Na^+ does not decrease below 2 once the ion is in the filter, except near the central binding site S_2, where the highest selectivity is observed (Fig. 5). These results suggest that selectivity is predominantly affected by the type of coordinating ligands (carbonyls *versus* water molecules) rather than by the total coordination number.

Conclusion

Extensive 3D umbrella sampling simulations were carried out in order to characterize the free energy landscapes governing the entry of extracellular Na^+ and K^+ into a KcsA selectivity filter occupied by two K^+. These calculations depend on the accuracy of the force field employed, which in our case is based on the all-atom PARAM22 potential energy function of CHARMM.[41] Comparison with the all-atom nonpolarizable AMBER force field[42] previously indicated that the general trends extracted from free energy perturbation simulations are consistently reproduced, with minor quantitative differences.[43] These types of force fields, which are based on effective fixed atomic partial charges, do not include polarizability explicitly, but only in an average way. While MD simulations based on effective additive force fields can still yield meaningful results for a broad range of biomolecular systems, the approximation has important consequences for ion–ligand energetics, and the results should be interpreted with caution.[44,45] Furthermore, the present calculations were carried out with the X-ray structure of KcsA, which has a closed intracellular gate. For this reason, it was possible to characterize the permeation process of a Na^+ only up to the middle of the selectivity filter, near site S_2. It will be possible to characterize the complete permeation process of a Na^+ all the way across the full selectivity filter using multi-ion PMF simulations from the extracellular side to the intracellular side with an open KcsA structure. One may note that, in this case, a fourth K^+ will be needed to enter the selectivity filter from the extracellular side to allow ion I_1 to move beyond S_2 and complete the inward permeation process. Characterizing the free energy landscape governing these additional steps shall be the object of future investigations when a high-resolution structure of the KcsA channel with the open state is available.

These limitations notwithstanding, the current PMF computations are able to capture important differences between the entry of a K^+ and the entry of a Na^+ into the selectivity filter under identical conditions, and a number of important observations can be made on the basis of those results. First, the depths of the free energy minima for the configurations [S_0, S_2, S_4] and [S_1, S_3, cavity] are similar in the $Na^+/K^+/K^+$ and $K^+/K^+/K^+$ systems. That is, the "thermodynamic" selectivity of binding sites S_0 and S_1 for K^+ over Na^+ is small, if at all existent. Second, the free energy barriers between the stable locations are generally higher for Na^+ than for K^+, whose energy landscape is smoother. This suggests that the translocation of Na^+ along the pore will be impeded and kinetically slower than K^+. This is in accord with a recent study combining crystallography and computations that also emphasized the importance of kinetic control on the selectivity of the KcsA channel.[26] Third, the region of binding site S_2 clearly displays more selectivity for K^+ over Na^+; a Na^+ faces a steep energy increase as it tries to cross this region of the pore. However, while S_2 is a stable location for K^+, it is not really a binding site for Na^+. Fourth, selectivity is not correlated with the overall coordination number around the ion entering the pore. Rather, it appears to be predominantly affected and modulated by changes in the type of coordinating ligands, as the water molecules are substituted by carbonyl oxygens.

These results further highlight the importance of the central region corresponding to binding site S_2 in the selectivity filter. Previous FEP/MD calculations showed this region to have the highest selectivity for K^+ over Na^+.[11,15] Now, extensive PMF calculations show that the multi-ion permeation process encounters an increasingly large free energy barrier as Na^+ attempts to move into the region of the S_2 site. The critical role of the S_2 region is also reflected in the pore structure of homologous

channels. For example, one of the main differences between the nonselective cationic NaK channel and the K^+-selective KcsA channel is the widening of the pore at the level of the central binding site S_2 in NaK.[46] This leads to the speculation that a loss of selectivity of site S_2 could be the principal reason that this channel is able to conduct Na^+, unlike KcsA,[47] which was later confirmed by all-atom FEP/MD simulations.[43] In addition, occupancy of binding site S_2 by K^+ has been linked to the ability of the selectivity filter to retain its conducting conformation by preventing the flipping of the Val76-Gly77 carbonyl group.[29,33] Annihilation of this site is also one of the hallmarks of the low-K pinched conformation.[3,24,28,32]

A consistent picture of ion selectivity in KcsA emerges from computational studies, whether relative free energies are probed for specific ion configurations via FEP/MD simulations[11,12,15] or mapped out in more detail via complete PMF umbrella sampling calculations such as those reported here. Overall, the outermost binding sites S_0 and S_1 do not appear to be very selective for K^+ over Na^+. Entry of a Na^+ into the selectivity filter is not thermodynamically unfavorable, at least not until the ion reaches the central region near binding site S_2. In part, the weak selectivity of the outermost sites may reflect the inaccuracies and limitations of a nonpolarizable force field. Nevertheless, previous experience with all-atom MD simulations suggests that the results should have semiquantitative accuracy.[45] Therefore, it is likely that the moderately low selectivity of the pore away from the central region is a robust conclusion that will not change, even with improved microscopic models and potential functions. It becomes increasingly important to fully exploit all available information about free energy variations along the selectivity filter in the KcsA channel to strengthen our confidence in the conclusions from the computations. One may anticipate the quantitative information deduced from the Ba^{2+} blockade, such as that previously carried out by Neyton and Miller for the MaxiK channel (BK),[21,22] to be particularly informative about KcsA. Similar Ba^{2+} blockade experiments on the KcsA channel are currently under way,[48] and with the availability of high-resolution X-ray structures of KcsA with bound Ba^{2+},[23,24] it shall soon be possible to undertake MD simulation studies based on models matching faithfully the conditions under which those experiments are carried out and to further deepen our understanding of selectivity in K^+ channels.

Methods

Two atomic systems similar to those used in previous studies[9,11,15] were simulated. Briefly, the first simulation system contains the tetrameric KcsA channel surrounded by 112 dipalmitoyl-phosphatidylcholine lipids (forming a bilayer), 6778 water molecules, and 21 Cl^- and 9 K^+ corresponding to a concentration of 150 mM KCl. The channel, taken from the high-resolution X-ray crystallographic structure of KcsA (PDB ID 1K4C),[3] is oriented parallel with the Z-axis of the simulation box. The X-ray structure corresponds to a conformation of the channel with its intracellular gate closed.[3] The first system is exposed only to K^+ ($K^+/K^+/K^+$), and the second system is nearly identical, with the outermost K^+ in the selectivity filter replaced by a Na^+ ($Na^+/K^+/K^+$).

All MD simulations were carried out using the program CHARMM,[49] together with the CHARMM PARAM22 protein force field[41] extended with the quantum mechanical phi–psi backbone dihedral potential Cmap,[50] the CHARMM PARAM27 lipid force field,[51] and the TIP3P water model.[52] Optimized parameters were used for K^+[53] and Na^+.[15] The length of chemical bonds involving hydrogen atoms was kept fixed using the SHAKE algorithm.[54] The systems were simulated with a time step of 2 fs, with periodic rectangular boundary conditions applied in all directions to simulate a multilayer system of membranes extending in the XY plane. The Z dimension of the unitary cell was allowed to vary according to the constant pressure and temperature thermodynamic ensemble with fixed XY surface area (CPTA).[51,55] Long-range electrostatic interactions in the periodic system were computed with the particle mesh Ewald method.[56]

Umbrella sampling simulations were performed with harmonic biasing potentials acting on the Z coordinates Z_1, Z_2, and Z_3 of the three ions in the KcsA selectivity filter region. This was performed as described by Bernèche and Roux.[11] The zero position along the Z-axis of the system corresponds to the center-of-mass of the backbone atoms of residues Thr75, Val76, Gly77, and Tyr78 (see Fig. 2). A harmonic potential with a force constant of 20 kcal/(mol Å^2) centered on specific values of $Z_1^{(i)}$, $Z_2^{(i)}$, and $Z_3^{(i)}$ was used for biasing window potentials.

The reference positions of the biasing potentials $Z_1^{(i)}$, $Z_2^{(i)}$, and $Z_3^{(i)}$ for the Z coordinates of the three ions were distributed over a 3D grid with a spacing of 0.5 Å. Based on this grid, three overlapping regions were sampled for each system: upper, central, and lower. The upper sampling region describes the process of ion I_1 entering from the extracellular side into binding site S_0 of the selectivity filter, while ion I_2 moves from binding site S_1 to S_2, and ion I_3 moves from S_3 to S_4 (see Fig. 2 for the location of the binding sites in the selectivity filter). For the $K^+/K^+/K^+$ system, this means that $Z_1^{(i)}$ was varied in 0.5 Å steps from 13.0 Å to 5.5 Å, $Z_2^{(i)}$ was varied in 0.5 Å steps from Min[5.5, $Z_1^{(i)}-3.5$] Å to −0.5 Å, and $Z_3^{(i)}$ was varied in 0.5 Å steps from Min[−0.5, $Z_2^{(i)}-4.5$] Å to −6.5 Å. This guarantees a minimum distance of 3.5 Å between ion I_1 and ion I_2, as well as a minimum distance of 4.5 Å between ion I_2 and ion I_3. The latter minimum distance was chosen to be a bit larger because ions I_2 and I_3 are located in the selectivity filter, where they are necessarily separated by a water molecule.

The central sampling region corresponds to the transition of ion I_1 from binding site S_0 to S_1, while ion I_2 goes from S_2 to S_3, and ion I_3 goes from S_4 to the aqueous cavity of the channel. For this region of the $K^+/K^+/K^+$ system to be sampled, $Z_1^{(i)}$ was varied in 0.5 Å steps from 8.0 Å to 2.5 Å, while $Z_2^{(i)}$ was varied in 0.5 Å steps from Min[2.5, $Z_1^{(i)}-4.5$] Å to −3.5 Å, and $Z_3^{(i)}$ was varied in 0.5 Å steps from Min[−2.5, $Z_2^{(i)}-3.5$] Å to −10.0 Å. The lower sampling region corresponds to the transition of ion I_1 from binding site S_1 to S_2, and ion I_2 from S_3 to S_4, while ion I_3 is essentially located in the aqueous cavity of the channel. For the sampling of the lower region of the $K^+/K^+/K^+$ system, $Z_1^{(i)}$ was varied from 5.0 Å to −0.5 Å, Z_2 was varied from Min[−0.5, $Z_1^{(i)}-4.5$] Å to −7.0 Å, and Z_3 was varied

from Min[−4.0, $Z_2^{(i)}$−3.5] Å to −14.0 Å. The three sampling regions of the $Na^+/K^+/K^+$ system were defined in a similar way. However, because Na^+ is smaller than K^+, the minimum distance between ion I_1 and ion I_2 was reduced by −0.5 Å, and the sampling regions of the coordinate Z_1 were shifted accordingly by −0.5 Å to ensure a better coverage of the sampling regions of the $Na^+/K^+/K^+$ system.

In both cases, a single umbrella sampling window simulation was generated for each of the overlapping grid points belonging to different regions, leading to a grand total of 3931 MD window simulations for each of the two systems. Every window was simulated for 0.2 ns, with the first 0.1 ns being used for equilibration and with the last 0.1 ns being used for sampling proper, for a total aggregate MD simulation time of 0.8 μs for each of the two systems. For comparison, the multi-ion PMF calculations reported previously by Bernèche and Roux were based on 308 MD simulations of 100 ps each, for a total aggregate time of about 30 ns.[11] The unbiased 3D PMF for the two systems were calculated using the weighted histogram analysis method (WHAM).[57,58] The width of the histogram bins was 0.1 Å. The WHAM equation was iterated 2000 times; the PMF varied by less than 0.2 kcal/mol between iteration cycle 1500 and iteration cycle 2000.

To facilitate the visualization of the free energy landscape governing the multi-ion translocation, we calculated reduced PMF maps depending on less than 3 degrees of freedom by numerical integration of the Boltzmann factor of the 3-ion PMF $W(Z_1,Z_2,Z_3)$. A first 2D PMF, $W(Z_1,Z_{23})$, depending on the position of the outermost ion I_1 and the average position of the two inner K^+, was calculated as:

$$e^{-W(Z_1,Z_{23})/k_BT} = \int dZ_2 \int dZ_3\, \delta[Z_{23} - (Z_2 + Z_3)/2]\, e^{-W(Z_1,Z_2,Z_3)/k_BT} \quad (1)$$

A second 2D PMF, $W(Z_1, Z_2)$, depending on the position of the outermost ion I_1 and the position of the center K^+, was calculated as:

$$e^{-W(Z_1,Z_2)/k_BT} = \int dZ_3\, e^{-W(Z_1,Z_2,Z_3)/k_BT} \quad (2)$$

In addition, a reduced one-dimensional free energy profile, $W(Z_1)$, depending only on the Z-position of the outermost ion, was calculated as:

$$e^{-W(Z_1)/k_BT} = \int dZ_2 \int dZ_3\, e^{-W(Z_1,Z_2,Z_3)/k_BT} \quad (3)$$

Those reduced PMF, which were calculated by numerical integration of three-ion PMF $W(Z_1, Z_2, Z_3)$, are displayed in the figures.

The average coordination numbers around the outermost ion, $N^{(i)}_{water}$, $N^{(i)}_{carbonyl}$, and $N^{(i)}_{total}$, were calculated for selected umbrella sampling windows. The average numbers of water and carbonyl oxygen atoms closer than 3.2 Å from ion I_1 in the $K^+/K^+/K^+$ system and closer than 2.8 Å in the $Na^+/K^+/K^+$ system were obtained from a set of 0.1 ns additional simulations per umbrella window. The atom coordinates of a simulation system were saved every 50 fs. In the case of K^+, one sampling window for every value of $Z_1^{(i)}$ between 13.0 Å and 0.0 Å (0.5 Å steps)—close to the dominant minimum free energy path of the corresponding 3D PMF—was chosen. For $Z_1^{(i)}$ between 13.0 Å and 7.0 Å, $Z_2^{(i)}$ was kept at 1.0 Å, and $Z_3^{(i)}$ was kept at −5.0 Å. This describes the entry of ion I_1 into the selectivity filter, while ion I_2 is in binding site S_2 and ion I_3 is in S_4. For $Z_1^{(i)}$ between 6.5 Å and 0.0 Å, $Z_2^{(i)}$ was set to $Z_1^{(i)}$−6.0 Å, and $Z_3^{(i)}$ was set to $Z_1^{(i)}$−12.0 Å, describing a single-file movement of all three ions deeper into the pore. In the case of Na^+, the values of $Z_2^{(i)}$ and $Z_3^{(i)}$ were the same as in the case of K^+, but $Z_1^{(i)}$ was reduced by −0.5 Å in order to account for the smaller average distance between I_1 and I_2. Simulations of neighboring windows along the chosen paths in the two systems sample an overlapping region. To account for the overlap, the average coordination number was calculated at position $Z = Z_1^{(i)}$ by smoothing over the neighboring sampling windows [i.e., $n^{(i)} = 0.25N^{(i-1)} + 0.5N^{(i)} + 0.25N^{(i+1)}$].

Acknowledgements

We thank Sergei Y. Noskov and Albert C. Pan for their help and support. Useful discussions with David Medovoy and Albert Lau are acknowledged. This work was funded by the National Institutes of Health through grant GM062342 and by a research fellowship from the Deutsche Forschungsgemeinschaft (German Research Foundation) to B.E. The computations were made possible by an allocation from the National Science Foundation through TeraGrid resources provided by the National Center for Supercomputing Applications.

References

1. Hille, B. (2001). Ionic Channels of Excitable Membranes, 3rd edit. Sinauer, Sunderland, MA.
2. Doyle, D., Cabral, J., Pfuetzner, R., Kuo, A., Gulbis, J., Cohen, S. *et al.* (1998). The structure of the potassium channel: molecular basis of K^+ conduction and selectivity. *Science*, **280**, 69–77.
3. Zhou, Y., Morais-Cabral, J. H., Kaufman, A. & MacKinnon, R. (2001). Chemistry of ion coordination and hydration revealed by a K^+ channel–Fab complex at 2.0 Å resolution. *Nature*, **414**, 43–48.
4. Heginbotham, L., Abramson, T. & MacKinnon, R. (1992). A functional connection between the pores of distantly related ion channels as revealed by mutant K^+ channels. *Science*, **258**, 1152.
5. Heginbotham, L., Lu, Z., Abramson, T. & Mackinnon, R. (1994). Mutations in the K^+ channel signature sequence. *Biophys. J.* **66**, 1061–1067.
6. Hille, B., Armstrong, C. M. & MacKinnon, R. (1999). Ion channels: from idea to reality. *Nat. Med.* **5**, 1105–1119.
7. Guidoni, L., Torre, V. & Carloni, P. (1999). Potassium and sodium binding to the outer mouth of the K^+ channel. *Biochemistry*, **38**, 8599–8604.
8. Allen, T. W., Bliznyuk, A., Rendell, A., Kuyucak, S. & Chung, S. H. (2000). The potassium channel: structure, selectivity and diffusion. *J. Chem. Phys.* **112**, 8191–8204.
9. Bernèche, S. & Roux, B. (2000). Molecular dynamics of the KcsA K(+) channel in a bilayer membrane. *Biophys. J.* **78**, 2900–2917.
10. Åqvist, J. & Luzhkov, V. B. (2000). Ion permeation mechanism of the potassium channel. *Nature*, **404**, 881–884.
11. Bernèche, S. & Roux, B. (2001). Energetics of ion conduction through the K^+ channel. *Nature*, **414**, 73–77.

12. Luzhkov, V. & Åqvist, J. (2001). K(+)/Na(+) selectivity of the KcsA potassium channel from microscopic free energy perturbation calculations. *Biochim. Biophys. Acta*, **1548**, 194–202.
13. Biggin, P. C., Smith, G. R., Shrivastava, I., Choe, S. & Sansom, M. S. (2001). Potassium and sodium ions in a potassium channel studied by molecular dynamics simulations. *Biochim. Biophys. Acta*, **1510**, 1–9.
14. Shrivastava, I. H., Tieleman, D. P., Biggin, P. C. & Sansom, M. S. (2002). K(+) *versus* Na(+) ions in a K channel selectivity filter: a simulation study. *Biophys. J.* **83**, 633–645.
15. Noskov, S., Bernèche, S. & Roux, B. (2004). Control of ion selectivity in K(+) channels by dynamic and electrostatic properties of carbonyl ligands. *Nature*, **431**, 830–834.
16. Sansom, M. S., Shrivastava, I. H., Bright, J. N., Tate, J., Capener, C. E. & Biggin, P. C. (2002). Potassium channels: structures, models, simulations. *Biochim. Biophys. Acta*, **1565**, 294–307.
17. Roux, B. (2005). Ion conduction and selectivity in K^+ channels. *Annu. Rev. Biophys. Biomol. Struct.* **34**, 153–171.
18. Noskov, S., Bernèche, S. & Roux, B. (2006). Ion selectivity in potassium channels. *Biophys. Chem.* **124**, 279–291.
19. Heginbotham, L., LeMasurier, M., Kolmakova-Partensky, L. & Miller, C. (1999). Single *Streptomyces lividans* K(+) channels. Functional asymmetries and sidedness of proton activation. *J. Gen. Physiol.* **114**, 551–560.
20. LeMasurier, M., Heginbotham, L. & Miller, C. (2001). KcsA: it's a potassium channel. *J. Gen. Physiol.* **118**, 303–314.
21. Neyton, J. & Miller, C. (1988). Potassium blocks barium permeation through a calcium-activated potassium channel. *J. Gen. Physiol.* **92**, 549–567.
22. Neyton, J. & Miller, C. (1988). Discrete Ba^{2+} block as a probe of ion occupancy and pore structure in the high-conductance Ca^{2+}-activated K^+ channel. *J. Gen. Physiol.* **92**, 569–586.
23. Jiang, Y. & MacKinnon, R. (2000). The barium site in a potassium channel by X-ray crystallography. *J. Gen. Physiol.* **115**, 269–272.
24. Lockless, S., Zhou, M. & MacKinnon, R. (2007). Structural and thermodynamic properties of selective ion binding in a K^+ channel. *PLoS Biol.* **5**, e121.
25. Nimigean, C. & Miller, C. (2002). Na(+) block and permeation in a K(+) channel of known structure. *J. Gen. Physiol.* **120**, 323–335.
26. Thompson, A. N., Kim, I., Panosian, T. D., Iverson, T. M., Allen, T. W. & Nimigean, C. M. (2009). Mechanism of potassium-channel selectivity revealed by Na(+) and Li(+) binding sites within the KcsA pore. *Nat. Struct. Mol. Biol.* **16**, 1317–1324.
27. Bernèche, S. & Roux, B. (2003). A microscopic view of ion conduction through the KcsA K^+ channel. *Proc. Natl Acad. Sci.* **100**, 8644–8648.
28. Domene, C. & Furini, S. (2009). Dynamics, energetics, and selectivity of the low-K^+ KcsA channel structure. *J. Mol. Biol.* **389**, 637–645.
29. Bernèche, S. & Roux, B. (2005). A gate in the selectivity filter of K^+ channels. *Structure*, **13**, 591–600.
30. Cordero-Morales, J., Cuello, L., Zhao, Y., Jogini, V., Cortes, D., Roux, B. & Perozo, E. (2006). Molecular determinants of gating at the potassium-channel selectivity filter. *Nat. Struct. Mol. Biol.* **13**, 311–318.
31. Cordero-Morales, J. F., Jogini, V., Lewis, A., Vásquez, V., Cortes, D. M., Roux, B. & Perozo, E. (2007). Molecular driving forces determining potassium channel slow inactivation. *Nat. Struct. Mol. Biol.* **14**, 1062–1069.
32. Domene, C., Vemparala, S., Furini, S., Sharp, K. & Klein, M. L. (2008). The role of conformation in ion permeation in a K^+ channel. *J. Am. Chem. Soc.* **130**, 3389–3398.
33. Valiyaveetil, F., Leonetti, M., Muir, T. & MacKinnon, R. (2006). Ion selectivity in a semisynthetic K^+ channel locked in the conductive conformation. *Science*, **314**, 1004–1007.
34. Roux, B., Allen, T. W., Bernèche, S. & Im, W. (2004). Theoretical and computational models of biological ion channels. *Q. Rev. Biophys.* **37**, 15–103.
35. Zwanzig, R. W. (2001). Nonequilibrium Statistical Mechanics. Oxford University Press, New York, NY.
36. Kirkwood, J. (1935). Statistical mechanics of fluid mixtures. *J. Chem. Phys.* **3**, 300–313.
37. Zhou, M. & MacKinnon, R. (2004). A mutant KcsA K(+) channel with altered conduction properties and selectivity filter ion distribution. *J. Mol. Biol.* **338**, 839–846.
38. Hodgkin, A. L. & Keynes, R. D. (1955). The potassium permeability of a giant nerve fibre. *J. Physiol. (London)*, **128**, 61–88.
39. Jensen, M. O., Borhani, D. W., Lindorff-Larsen, K., Maragakis, P., Jogini, V., Eastwood, M. P. *et al.* (2010). Principles of conduction and hydrophobic gating in K^+ channels. *Proc. Natl Acad. Sci. USA*, **107**, 5833–5838.
40. Humphrey, W., Dalke, A. & Schulten, K. (1996). VMD: Visual Molecular Dynamics. *J. Mol. Graphics*, **14**, 33–38.
41. MacKerell, Jr., A. J., Bashford, D., Bellot, M., Dunbrack, R., Evanseck, J., Field, M. *et al.* (1998). All-atom empirical potential for molecular modeling and dynamics studies of proteins. *J. Phys. Chem. B*, **102**, 3586–3616.
42. Cornell, W., Cieplak, P., Bayly, C., Gould, I., Merz, K., Jr, Ferguson, D. *et al.* (1995). A second generation force field for the simulation of proteins and nucleic acids. *J. Am. Chem. Soc.* **117**, 5179–5197.
43. Noskov, S. & Roux, B. (2007). Importance of hydration and dynamics on the selectivity of the KcsA and NaK channels. *J. Gen. Physiol.* **129**, 135–143.
44. Roux, B. & Karplus, M. (1995). Potential energy function for cations–peptides interactions: an ab initio study. *J. Comput. Chem.* **16**, 690–704.
45. Roux, B. & Bernèche, S. (2002). On the potential functions used in molecular dynamics simulations of ion channels,. *Biophys. J.* **82**, 1681–1684.
46. Shi, N., Ye, S., Alam, A., Chen, L. & Jiang, Y. (2006). Atomic structure of a Na^+- and K^+-conducting channel. *Nature*, **440**, 570–574.
47. Zagotta, W. (2006). Membrane biology: permutations of permeability. *Nature*, **440**, 427–429.
48. Piasta, K. & Miller, C. (2010). Probing the KcsA permeation pathway using barium Block. *Biophys. J.* **96**, 179a.
49. Brooks, B. R., Brooks, C. L., III, Mackerell, Jr., A. D., Nilsson, L., Petrella, R. J., Roux, B. *et al.* (2009). CHARMM: the biomolecular simulation program. *J. Comput. Chem.* **30**, 1545–1614, doi:10.1002/jcc.21287.
50. MacKerell, Jr., A. D., Feig, M. & Brooks, C., III (2004). Improved treatment of the protein backbone in empirical force fields. *J. Am. Chem. Soc.* **126**, 698–699.
51. Feller, S., Venable, R. & Pastor, R. (1997). Computer simulation of a DPPC phospholipid bilayer. Structural changes as a function of molecular surface area. *Langmuir*, **13**, 6555–6561.

52. Jorgensen, W. L., Chandrasekhar, J., Madura, J. D., Impey, R. W. & Klein, M. L. (1983). Comparison of simple potential functions for simulating liquid water. *J. Chem. Phys.* **79**, 926–935.
53. Beglov, D. & Roux, B. (1994). Finite representation of an infinite bulk system: solvent boundary potential for computer simulations. *J. Chem. Phys.* **100**, 9050–9063.
54. Ryckaert, J., Ciccotti, G. & Berendsen, H. (1977). Numerical integration of the Cartesian equation of motions of a system with constraints: molecular dynamics of *n*-alkanes. *J. Comput. Chem.* **23**, 327–341.
55. Feller, S., Zhang, Y., Pastor, R. & Brooks, B. (1995). Constant pressure molecular dynamics simulation—the Langevin piston method. *J. Chem. Phys.* **103**, 4613–4621.
56. Essmann, U., Perera, L., Berkowitz, M., Darden, T., Lee, H. & Pedersen, L. (1995). A smooth particle mesh Ewald method. *J. Chem. Phys.* **103**, 8577–8593.
57. Kumar, S., Bouzida, D., Swendsen, R., Kollman, P. & Rosenberg, J. (1992). The Weighted Histogram Analysis Method for free-energy calculations on biomolecules: I. The method. *J. Comput. Chem.* **13**, 1011–1021.
58. Roux, B. (1995). The calculation of the potential of mean force using computer simulations. *Comput. Phys. Commun.* **91**, 275–282.